$1n$-decay cross-section of superheavy nuclei with Z_{CN}=102-113 using hot and cold orientations

Gurjit Kaur, Kirandeep Sandhu, and Manoj K. Sharma*
School of Physics and Materials Science,
Thapar University, Patiala 147004, Punjab, INDIA

Introduction

The quest to synthesize new elements with Z≥101 is materialized using the heavy ion-induced reaction dynamics. Within this interaction process,the superheavy elements lying in range Z=102-113 are synthesized within the cold fusion reactions, whereas the formation of Z≥114 is carried out using the well-known hot fusion process. In cold fusion synthesis, usually ^{208}Pb and ^{209}Bi target nuclei are bombarded with neutron rich projectiles having masses in the range A_2=50-70. These reactions are characterized by low excitation energies accompanied via 1 or 2 neutron(s) emission. Hence high survival probability is expected for compound nucleus formed within the cold fusion process. On the other hand, this interaction process has limited scope of extension, because as Z_{CN} increases, the production cross-sections of evaporation residues decrease sharply. The decrement in cross-section is due to the competing role of other processes like quasi-fission in the competition with complete fusion.

In view of the above discussion, the dynamics involved in the cold fusion reactions is studied within the framework of the dynamical cluster decay model (DCM) [1, 2]. In this work, $1n$-decay of Z_{CN}=102-113 [3] is visualized by using β_{2i}-deformations within the optimum orientation approach. It is relevant to mention that, in DCM, the optimum orientations are assigned for polar (or elongated) and equatorial (or compact), respectively, for configurations corresponding to largest interaction radius with lowest barrier and smallest interaction radius with highest barrier [1].

*Electronic address: msharma@thapar.edu

The Model

The dynamical cluster decay model [1, 2] based on fragmentation theory is worked out in terms of mass or charge asymmetry, relative separation $\bar{R}$, neck parameter, deformation and orientation. In terms of these parameters and for proper inclusion of temperature effect, the fragmentation potential V(η,R) reads as:-

$$\begin{aligned} V(\eta,R) &= \sum_{i=1}^{2} V_{LDM}(A_i,Z_i,T) \\ &+ \sum_{i=1}^{2} \delta U_i \exp(-T^2/T_0^2) \\ &+ V_C(R,Z_i,\beta_{\lambda i},\theta_i,T) \\ &+ V_P(R,A_i,\beta_{\lambda i},\theta_i,T) \\ &+ V_\ell(R,A_i,\beta_{\lambda i},\theta_i,T). \end{aligned} \quad (1)$$

Using above potential, the Schrödinger wave equation is solved in η-coordinates at fixed R=R$_a$:

$$\left[-\frac{\hbar^2}{2\sqrt{B_{\eta\eta}}}\frac{\partial}{\partial\eta}\frac{1}{\sqrt{B_{\eta\eta}}}\frac{\partial}{\partial\eta}+V(\eta)\right]\psi^\nu(\eta)=E_\eta^\nu\psi^\nu(\eta), \quad (2)$$

to get the preformation probability:

$$P_0 = \mid \psi(\eta(A_i)) \mid^2 \sqrt{B_{\eta\eta}}\frac{2}{A_{CN}}, \quad (3)$$

The barrier penetrability(P) of the decaying fragments is worked out using WKB approach.

Calculations and discussion

In this work the theoretical analysis of experimental data for Z_{CN}=102-113 nuclei [3] is carried out within the DCM framework, using optimum orientations and β_{2i}-deformed fragmentation. It is relevant to mention that we have studied $1n$-decay for a wide range of nuclei i.e. Z_{CN}=102-113,

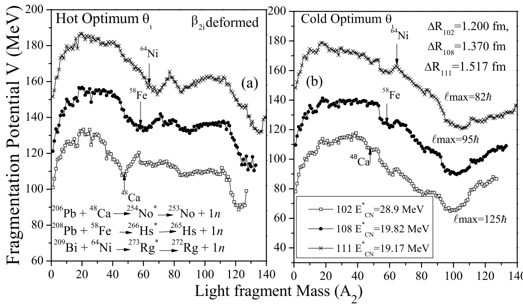

FIG. 1: Comparison of fragmentation potential at maximum energy for $1n$-decay of No, Hs, Rg nuclei (a) for hot orientation and (b) for cold orientation approaches.

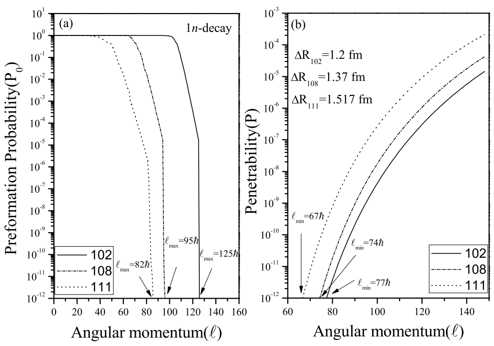

FIG. 2: Variation of preformation probability and penetrability as a function of angular momentum for No, Hs, Rg nuclei.

but here we have presented the work only for Z_{CN}=102(No), 108(Hs) and 111(Rg), so that an overview of the cold fusion reaction dynamics can be extracted. Fig.1 is plotted to optimize the best possible orientation approach for these reactions. This figure clearly signifies that in the fragmentation potential of ^{254}No*, ^{266}Hs* and ^{273}Rg* decaying nuclei, the minima around the entrance channel i.e. ^{206}Pb+^{48}Ca, ^{208}Pb+^{58}Fe and ^{209}Bi+^{64}Ni is observed for the hot optimum orientation approach, which is governed through smallest interaction radius with highest barrier. Hence one may conclude that, to address the $1n$-decay observed in usual cold fusion reactions, the hot-compact orientation seems to be more favourable as compared to the anticipated cold-elongated configuration.

Further to explore the dynamics involved through the hot orientation approach, Fig.2 is plotted. This figure shows the variation of preformation probability and barrier penetrability as a function of angular momentum for the $1n$-decay of ^{254}No*, ^{266}Hs* and ^{273}Rg* compound nuclei. In panel (a) we can see that the preformation probability for $1n$-decay remains almost constant for significance range of angular momentum, and finally decreases to zero near ℓ_{max}-state. Another important point regarding the Fig.2(a) lies in the fact that the drop in the preformation factor occurs earlier for the higher-Z nucleus. It is relevant to mention that preformation probability represents the likelihood of formation of decaying fragments at compound nucleus stage and imparts much needed structure related information. The other factor which contributes towards cross-sections is the barrier penetrability, shown in panel (b). Antithetical to P_0, the value of P increases with increase in angular momentum and remains higher for ^{273}Rg* followed by ^{266}Hs* and ^{254}No*. The information depicted in Fig.2 can be used to find the upper and lower limits of angular momentum contributing toward the channel cross-sections.

Summarizing above, hot optimum orientations are more favourable to address $1n$-decay of Z_{CN}=102-113 superheavy nuclei, formed in cold fusion reactions. In addition to this, ℓ-window is decided from the preformation and the penetration probability plots, which in turn help to estimate the channel cross-sections. Also, for increasing ℓ-value, the behavior of P_0 and P exhibit opposite pattern and hence role of these quantities be dealt with care in order to have overall analysis of heavy ion induced reaction dynamics.

References

[1] K. Sandhu, M. K. Sharma, R. K. Gupta, Phys. Rev. C **86**, 064611 (2012).

[2] K. Sandhu, M. K. Sharma, R. K. Gupta, Phys. Rev. C **90**, 034610 (2014).

[3] K. Morita et. al., Journal of Physical Society of Japan **73**, 2593-2596 (2004).